

Template Removal and Thermal Stability of Organically Functionalized Mesoporous Silica Nanoparticles

Rajeev Kumar,[†] Hung-Ting Chen,^{†,‡} Juan L. V. Escoto,[‡] Victor S.-Y. Lin,^{*,†,‡} and Marek Pruski^{*,†}

Ames Laboratory (United States Department of Energy) and Department of Chemistry, Iowa State University, Ames, Iowa 50011-3020

Received March 12, 2006. Revised Manuscript Received June 23, 2006

The surfaces of organically functionalized, MCM-41-type mesoporous silica nanoparticle materials, prepared by a co-condensation method, were studied by solid-state nuclear magnetic resonance (NMR) spectroscopy following a series of heat treatments between 100 and 400 °C. The surfaces were functionalized with 2,2'-bipyridine, 4-(dimethylamino)pyridine, and pentafluorobenzene. The ¹³C and ²⁹Si NMR spectra of these materials showed that the structures and concentrations of these functional groups remained unaffected by the heat treatment. Furthermore, it has been demonstrated that the surfactant template, cetyltrimethylammonium bromide (CTAB), could be effectively removed from these materials by heat treatment without disrupting the covalent bonds between the functional groups and the silica surface. The chemical accessibility and reactivity of the organic functionalities were also preserved after heating.

1. Introduction

Since the discovery of the M41S family of mesoporous materials by Mobil scientists in 1992,^{1,2} extensive studies have been performed by research groups worldwide on the synthesis and applications of these materials in fields such as sorption, separation, sensor, delivery, and electronics.^{3–8} Also, these materials provide uniform porous structures with high surface area and tunable morphology that are highly desirable for selective heterogeneous catalysis. The major challenge that hindered the utilization of mesoporous silica-based catalysts in industrial processes involved the synthetic methods for surface functionalization with control of spatial distribution and adequate thermal stability. Recently, significant progress in the area of functionalization of MCM and SBA types of mesoporous silicas with catalytically active organic groups has been demonstrated,^{3,9–15} which resulted

in the synthesis of efficient and highly selective catalysts for several industrially relevant reactions.^{16–18}

Among the state-of-the-art methods for the surface functionalization of mesoporous silicas, the co-condensation of silicate with various organoalkoxysilanes has been shown to yield materials with a homogeneous spatial distribution of organic groups. To preserve the organic functional groups, the low-temperature processes, such as solvent extraction,^{19,20} have been widely used for template removal. These methods, on the other hand, often require the use of large volumes of organic solvents, and therefore cannot meet the economic and environmental constraints imposed by large-scale applications. Furthermore, several recent reports have indicated that the as-synthesized organically functionalized mesoporous silicas prepared by the solvent extraction methods lack the high hydrothermal stability that is necessary for some industrially important processes.^{21,22} This has been attributed to the defect sites created during the synthesis and/or the template-removal process of these materials.

* To whom correspondence should be addressed. Phone: (515) 294-2017 (M.P.); (515) 294-3135 (V.S.-Y.L.). E-mail: mpruski@iastate.edu (M.P.); vsylin@iastate.edu (V.S.-Y.L.).

[†] Ames Laboratory, Iowa State University.

[‡] Department of Chemistry, Iowa State University.

- (1) Kresge, C. T.; Leonowicz, M. E.; Roth, W. J.; Vartuli, J. C.; Beck, J. S. *Nature* **1992**, *359*, 710–712.
- (2) Beck, J. S.; Vartuli, J. C.; Roth, W. J.; Leonowicz, M. E.; Kresge, C. T.; Schmitt, K. D.; Chu, C. T. W.; Olson, D. H.; Sheppard, E. W.; McCullen, S. B.; Higgins, J. B.; Schlenker, J. L. *J. Mater. Chem.* **1992**, *114*, 10834–10843.
- (3) Corma, A. *Chem. Rev.* **1997**, *97*, 2373–2419.
- (4) Stein, A. *Adv. Mater.* **2003**, *15*, 763–775.
- (5) Lin, V. S. Y.; Lai, C.-Y.; Huang, J.; Song, S.-A.; Xu, S. *J. Am. Chem. Soc.* **2001**, *123*, 11510–11511.
- (6) Lai, C.-Y.; Trewyn, B. G.; Jeftinija, D. M.; Jeftinija, K.; Xu, S.; Jeftinija, S.; Lin, V. S. Y. *J. Am. Chem. Soc.* **2003**, *125*, 4451–4459.
- (7) Trewyn, B. G.; Whitman, C. M.; Lin, V. S. Y. *Nano Lett.* **2004**, *4*, 2139–2143.
- (8) Giri, S.; Trewyn, B. G.; Stellmaker, M. P.; Lin, V. S. Y. *Angew. Chem., Int. Ed.* **2005**, *44*, 5038–5044.
- (9) Stein, A.; Melde, B. J.; Schroden, R. C. *Adv. Mater.* **2000**, *12*, 1403–1419.
- (10) Clark James, H. *Acc. Chem. Res.* **2002**, *35*, 791–797.

- (11) Huh, S.; Wiench, J. W.; Yoo, J.-C.; Pruski, M.; Lin, V. S. Y. *Chem. Mater.* **2003**, *15*, 4247–4256.
- (12) Huh, S.; Wiench, J. W.; Trewyn, B. G.; Song, S.; Pruski, M.; Lin, V. S. Y. *Chem. Commun.* **2003**, 2364–2365.
- (13) Melero, J. A.; Stucky, G. D.; van Grieken, R.; Morales, G. *J. Mater. Chem.* **2002**, *12*, 1664–1670.
- (14) Hiyoshi, N.; Yogo, K.; Yashima, T. *Microporous Mesoporous Mater.* **2005**, *84*, 357–365.
- (15) Ford, D. M.; Simanek, E. E.; Shantz, D. F. *Nanotechnology* **2005**, *16*, 458–475.
- (16) Huh, S.; Chen, H.-T.; Wiench, J. W.; Pruski, M.; Lin, V. S. Y. *J. Am. Chem. Soc.* **2004**, *126*, 1010–1011.
- (17) Huh, S.; Chen, H.-T.; Wiench, J. W.; Pruski, M.; Lin, V. S. Y. *Angew. Chem., Int. Ed.* **2005**, *44*, 1826–1830.
- (18) Chen, H.-T.; Huh, S.; Wiench, J. W.; Pruski, M.; Lin, V. S. Y. *J. Am. Chem. Soc.* **2005**, *127*, 13305–13311.
- (19) Tanev, P. T.; Pinnavaia, T. J. *Chem. Mater.* **1996**, *8*, 2068–2079.
- (20) Zhao, X. S.; Lu, G. Q.; Whittaker, A. K.; Millar, G. J.; Zhu, H. Y. *J. Phys. Chem. B* **1997**, *101*, 6525–6531.
- (21) Igarashi, N.; Hashimoto, K.; Tatsumi, T. *J. Mater. Chem.* **2002**, *12*, 3631–3636.

Recent studies on the hydrothermal treatments of several nonfunctionalized mesoporous silica materials have demonstrated that, by controlling the temperature and moisture content, these processes could not only effectively remove template molecules, but also “cure” the defects and strengthen the structure stability of the mesoporous silica framework.^{22–28} However, to the best of our knowledge, no studies have been reported on using these methods for the template removal of organically functionalized mesoporous silica materials prepared by the co-condensation method.

Herein, we report on a systematic investigation of the thermal treatments of three mesoporous silica nanoparticle (MSN) materials that are functionalized with 4,4'-di-[(*N*-propyl)aminocarbonyl]-2,2'-bipyridine (BPY), 3-(pentafluorophenyl)propyl (PFP), and 4-[*N*-propyl-*N*-methyl-amino]pyridine (DMAP) groups. These MSNs were synthesized via the co-condensation method templated by CTAB surfactant micelles^{11,12,18,29,30} and characterized using a combination of solid-state NMR, X-ray diffraction, nitrogen adsorption, and fluorescence spectroscopy. The different organic groups were chosen to represent the common metal-binding ligands, the Lewis acids, and the nucleophilic catalytic functionalities, respectively. The structures and concentrations of surfactant molecules and the functional groups were monitored following a series of thermal treatments between 100 and 400 °C. Our primary analytical tool was solid-state NMR spectroscopy, which has outstanding applicability for silica surface characterization, especially in mesoporous materials.^{29–36} We have demonstrated that it is possible to efficiently remove the CTAB template molecules from the mesopores while fully preserving the chemical fidelity of the organic functional groups. The chemical accessibility and catalytic reaction studies are fully consistent with spectroscopic characterization before and after thermal treatments.

2. Experimental Section

2.1. Sample Synthesis. All reagents and chemicals were used as received from commercial vendors without any further purification.

- (22) Cassiers, K.; Linssen, T.; Mathieu, M.; Benjelloun, M.; Schrijnemakers, K.; Van Der Voort, P.; Cool, P.; Vansant, E. F. *Chem. Mater.* **2002**, *14*, 2317–2324.
- (23) Zhang, F.; Yan, Y.; Yang, H.; Meng, Y.; Yu, C.; Tu, B.; Zhao, D. *J. Phys. Chem. B* **2005**, *109*, 8723–8732.
- (24) Kim, J. M.; Jun, S.; Ryoo, R. *J. Phys. Chem. B* **1999**, *103*, 6200–6205.
- (25) Ryoo, R.; Jun, S. *J. Phys. Chem. B* **1997**, *101*, 317–320.
- (26) Kruk, M.; Jaroniec, M.; Sayari, A. *Microporous Mesoporous Mater.* **1999**, *27*, 217–229.
- (27) Igarashi, N.; Koyano, K. A.; Tanaka, Y.; Nakata, S.; Hashimoto, K.; Tatsumi, T. *Microporous Mesoporous Mater.* **2003**, *59*, 43–52.
- (28) Pauly, T. R.; Petkov, V.; Liu, Y.; Billinge, S. J. L.; Pinnavaia, T. J. *J. Am. Chem. Soc.* **2002**, *124*, 97–103.
- (29) Trebosc, J.; Wiench, J. W.; Huh, S.; Lin, V. S. Y.; Pruski, M. *J. Am. Chem. Soc.* **2005**, *127*, 3057–3068.
- (30) Trebosc, J.; Wiench, J. W.; Huh, S.; Lin, V. S. Y.; Pruski, M. *J. Am. Chem. Soc.* **2005**, *127*, 7587–7593.
- (31) Camus, L.; Goletto, V.; Maquet, J.; Gervais, C.; Bonhomme, C.; Babonneau, F.; Massiot, D. *J. Sol–Gel Sci. Technol.* **2003**, *26*, 311–314.
- (32) Shenderovich, I. G.; Buntkowsky, G.; Schreiber, A.; Gedat, E.; Sharif, S.; Albrecht, J.; Golubev, N. S.; Findenegg, G. H.; Limbach, H.-H. *J. Phys. Chem. B* **2003**, *107*, 11924–11939.
- (33) Christiansen, S. C.; Zhao, D.; Janicke, M. T.; Landry, C. C.; Stucky, G. D.; Chmelka, B. F. *J. Am. Chem. Soc.* **2001**, *123*, 4519–4529.
- (34) Alam, T. M.; Fan, H. *Macromol. Chem. Phys.* **2003**, *204*, 2023–2030.
- (35) Hagaman, E. W.; Zhu, H.; Overbury, S. H.; Dai, S. *Langmuir* **2004**, *20*, 9577–9584.

tion. Cetyltrimethylammonium bromide (CTAB), tetraethoxysilane (TEOS), and *cis*-bis(2,2'-bipyridine)dichlororuthenium(II) hydrate (Ru(bpy)₂Cl₂·xH₂O) were purchased from Aldrich. 3-(Pentafluorophenyl)propyltrimethoxysilane (PFP-TMS) was purchased from Gelest. The DMAP-MSN material and the pertinent 4-[*N*-[3-(triethoxysilyl)propyl]-*N*-methyl-amino]pyridine (DMAP-TES) were synthesized according to the procedures described in our previous paper.¹⁸ The 2,2'-bipyridyl-4,4'-dicarboxylic acid was prepared on the basis of a literature-reported procedure.³⁷ The nonfunctionalized MCM-41 silica and DMAP-MSN were synthesized following the procedures reported previously.¹⁸

Preparation of 4,4'-di-[*N*-[3-(trimethoxysilyl)propyl]aminocarbonyl]-2,2'-bipyridine (BPY-TMS). A solution of 2,2'-bipyridyl-4,4'-dicarboxylic acid (960 mg, 3.93 mmol) and excess thionyl chloride (20 mL) was refluxed for 3 h to yield the desired acid chloride. The reaction mixture was allowed to cool to room temperature. The unreacted thionyl chloride was removed by the rotary evaporator. The resulting crude 2,2'-bipyridyl-4,4'-dicarboxylic acid chloride was redissolved in a solution of benzene (160 mL) and pyridine (1.0 mL), followed by the addition of 3-aminopropyl trimethoxysilane (1.5 mL, 8.5 mmol). The mixture was allowed to reflux for 12 h. The solid precipitate was formed and removed by filtration to yield a pink solution. The filtrate was centrifuged to separate the pink impurity from the solution. The clear solution was decanted and concentrated in vacuo to give 788 mg (1.39 mmol, 35%) of BPY-TMS as a white solid powder. ¹H NMR (CDCl₃, 300 MHz): δ 8.72 (d, 2H), 8.68 (s, 2H), 7.80 (d, 2H), 6.96 (s, 2H), 3.54 (s, 18H), 3.50 (m, 4H), 1.78 (m, 4H), 0.74 (t, 4H). ¹³C NMR (CDCl₃, 75 MHz): δ 165.7 (CONH), 156.2, 150.3, 143.4, 122.5, 117.7, 50.9, 42.7, 22.8, 6.9. IR (KBr, cm⁻¹): 3342, 3052, 1646, 1545, 1313, 1077. MS (EI) *m/z*: 567 [M]⁺. HRMS calcd for C₂₄H₃₈N₄O₈-Si₂ 566.2228, found 566.2235.

Synthesis of 2,2'-Bipyridine-Functionalized Mesoporous Silica Nanoparticle (BPY-MSN) Material. A mixture of CTAB (1.0 g, 2.75 mmol), 2.0 M of NaOH (aq) (3.5 mL, 7.0 mmol), and H₂O (480 g, 26.67 mol) was heated to 80 °C for 30 min. TEOS (5 mL, 22.4 mmol) was first introduced dropwise to the CTAB solution, followed by the slow addition of BPY-TMS (0.543 g, 0.958 mmol). The mixture was stirred vigorously at 80 °C for 2 h followed by a hot filtration of the solution to yield the crude BPY-MSN product (white solid). The as-synthesized material was washed with copious amounts of water and methanol and then dried under vacuum. A surfactant-extracted BPY-MSN material was obtained by the acid extraction. In a typical procedure, as-synthesized BPY-MSN material (1.0 g) was treated with a methanolic solution (100 mL) of concentrated hydrochloric acid (1.0 mL) under reflux condition for 6 h, followed by filtration, extensive washing with water and methanol, and drying under vacuum.

Synthesis of Pentafluorobenzene-Functionalized Mesoporous Silica Nanoparticle (PFP-MSN) Material. As mentioned above, a mixture of CTAB (1.0 g, 2.75 mmol), 2.0 M of NaOH (aq) (3.5 mL, 7.0 mmol), and H₂O (480 g, 26.67 mol) was heated to 80 °C for 30 min. Two alkoxysilanes, TEOS (5 mL, 22.4 mmol) and PFP-TMS (0.58 mL, 2.24 mmol), were sequentially added to the surfactant solution via injection. A white precipitate was observed within 30 s upon mixing of the initial opaque emulsion. The mixture was stirred at 80 °C for 2 h, followed by a hot filtration to yield the as-synthesized PFP-MSN material. The material was washed extensively with copious amounts of water and methanol and then dried under vacuum. The acid extraction of CTAB surfactant from

- (36) Maciel, G. E. In *Encyclopedia of Nuclear Magnetic Resonance*; Grant, M. D., Harris, R. K., Eds.; John Wiley & Sons Ltd: Chichester, U.K., 1996; Vol. 7, p 4370.
- (37) Garelli, N.; Vierling, P. *J. Org. Chem.* **1992**, *57*, 3046–3051.

as-made material was performed by the aforementioned experimental condition to obtain a surfactant-extracted PFP-MSN sample.

2.2. Heat Treatment. The as-synthesized and surfactant-extracted silicas in their initial state will be referred to as BPY-as-RT, BPY-ex-RT, DMAP-as-RT, etc. The first series of thermally treated samples, which we denote BPY-as-100, BPY-ex-100, DMAP-as-100, etc., was obtained by placing the materials in glass tubes and evacuating to 1×10^{-5} Torr overnight at $T_c = 100$ °C. After the NMR measurements, the same samples were exposed to subsequent heat treatments at 150, 200, 225, 250, 282, and 350–400 °C, carried out for 2 h under the same pressure of 1×10^{-5} Torr. Again, each thermal treatment was followed by an NMR analysis. The nonfunctionalized MCM-41 samples were treated only at 100 and 400 °C in the as-synthesized state. To prevent rehydration, we handled the samples in a glovebag under dry nitrogen and measured them in tightly capped MAS rotors.

2.3. Characterization of MSN Materials. The particle morphology of MSNs was determined by scanning electron microscopy (SEM) with a JEOL 840A instrument. Powder XRD experiments were performed on a Scintag XDS 2000 diffractometer by scanning the 2θ angle between 1 and 10° and using a Cu K α radiation source. The surface area and median pore diameter were determined by N₂ adsorption/desorption measurements in a Micromeritics ASAP 2000 surface analyzer. Samples were prepared by degassing at 90 °C for 4 h before the measurements. The data were evaluated by Brunauer–Emmett–Teller (BET) and Barrett–Joyner–Halenda (BJH) methods to calculate the surface area and pore volumes/pore size distributions, respectively.

2.4. NMR. ¹³C and ²⁹Si solid-state NMR experiments were performed on a Varian/Chemagnetics Infinity 400 spectrometer equipped with a 5 mm Chemagnetics magic angle spinning (MAS) probe operated at a rate of 10 kHz. The ¹³C experiments, which used cross polarization (CP) from the nearby protons, were focused on monitoring the changes in the structure and concentration of molecules inside the mesopores as a function of T_c . During the CP period of 1.5 ms, the ¹H RF magnetic field ν_{RF}^H was ramped between 19 and 30 kHz using 1 kHz increments, whereas the ¹³C RF field ν_{RF}^C was maintained at a constant level of 30 kHz. The magnetic fields ν_{RF}^H of 70 and 50 kHz were used for initial excitation and during continuous wave decoupling, respectively. A total of 42 spectra were acquired (six samples treated at seven temperatures), each consisting of 12 000 scans, using a repetition time of 1.2 s. It is noted that direct polarization (DP), which is the preferred method in applications involving quantitative measurements, could not be used in this study because of prohibitively long relaxation delays, on the order of several minutes, associated with ¹³C nuclei. The CPMAS NMR method, on the other hand, yielded spectra that are not quantitative, because the observed ¹³C magnetizations were influenced by site-dependent ¹H–¹³C distances, relaxation processes, and molecular motions. However, we could still accurately monitor the relative changes in concentrations of functional groups as a function of T_c by acquiring each CPMAS NMR spectrum under identical conditions. To maximize the accuracy, we have verified the magnitudes of the applied RF fields between the measurements within each series of spectra using a reference sample. The changes in mobility of chemisorbed species due to the reconstruction (dehydroxylation) of the silica surface at higher temperatures may be the main source of error in these measurements.

The ²⁹Si DPMAS NMR experiments were performed in order to compare the surface functionalities after the final treatment with those present in the starting samples. For each sample, 300 scans were collected using ¹H TPPM decoupling³⁸ at $\nu_{RF}^H = 45$ kHz using a phase separation of 15°. The saturation recovery experiment

showed that the values of T_1 relaxation times for the silicon groups varied between 30 and 60 s. Therefore, a pulse delay of 300 s was chosen to ensure sufficient restoration of the initial ²⁹Si magnetization. All chemical shifts were referenced to SiMe₄ at 0 ppm.

The solution-state spectra reported in this work were acquired on a Varian VRX-300 spectrometer.

2.5. Chemical Accessibility and Reactivity Test of BPY-MSNs. BPY-as-350 or BPY-ex-RT material (50 mg) was suspended in a 10 mL ethanol solution of *cis*-bis(2,2'-bipyridine)dichlororuthenium(II) hydrate (0.337 mM) and refluxed for 12 h. The supernatant was isolated by filtration and diluted with ethanol to 50 mL. The amount of unreacted Ru(bpy)₂Cl₂·xH₂O in the supernatant was determined by measuring the UV/vis absorbance of the λ_{max} ($\epsilon = 3199.1 \text{ cm}^{-1} \text{ M}^{-1}$) at 365 nm in ethanol. The amount of chemically accessible 2,2'-bipyridine groups in BPY-as-350 and BPY-ex-RT was calculated by subtracting the amount of unreacted Ru(bpy)₂Cl₂·xH₂O from the initial concentration (0.337 mM). Also, the material obtained after reaction with Ru(bpy)₂Cl₂·xH₂O was carefully examined by measuring fluorescence spectra of MSNs suspended in the ethanol solution. The spectra were taken using excitation at 450 nm, an average wavelength of the MLCT band of a ruthenium(II) trispyridine complex.

In addition, we performed the Cu(II) adsorption capacity test on the same samples by following a literature-reported method.^{11,12,39} It was carried out by using 0.01 M Cu(NO₃)₂·2.5H₂O in 0.1 M tris(hydroxymethyl)aminomethane (trizma) solution and a contact time of 1 h. The amount of nonadsorbed Cu(II) ions in the filtrate was measured using a UV/vis spectrophotometer at $\lambda_{max} = 601$ nm.

2.6. Catalytic Reactivity Test of DMAP-as-400. A solution of 4-nitrobenzaldehyde (37.8 mg, 0.25 mmol) and DMAP-as-400 (50 mg, 0.075 mmol) in water/tetrahydrofuran (THF) (2 mL, 1/3 v/v) was charged to a screw-capped test tube, followed by the addition of methyl vinyl ketone (41.0 μ L, 0.5 mmol). The mixture was stirred at 50 °C for 24 h. The catalyst was separated by filtration and washed with acetone. The filtrate was collected and concentrated in vacuo to yield a yellow liquid. The crude was purified by the chromatography with an eluent of ethyl acetate/hexane (5/5 v/v) to yield 49.8 mg (0.225 mmol, 90%) of the purified product.

3. Results and Discussion

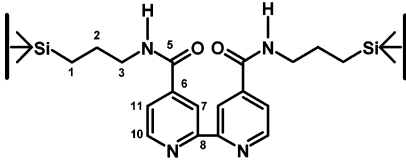
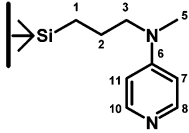
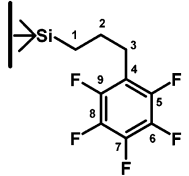
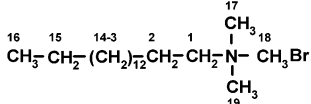
3.1. Solid-State NMR Characterization. The organically functionalized MSNs were thermally treated between 100 and 400 °C, as detailed in section 2.2, and the resulting materials were analyzed by solid-state NMR spectroscopy. The ¹³C CPMAS NMR spectra of functionalized samples showed that they contained the intended structures, i.e., the observed ¹³C chemical shifts closely matched those in the solution NMR spectra of respective functional groups. These structures are shown in Table 1, along with the site assignments, which will be further used in the discussion below. To separate the resonances representing functional groups from those due to CTAB, we measured the ¹³C CPMAS NMR spectrum of a nonfunctionalized sample MCM-as-100, which is shown and assigned in Figure 1.

3.1.1. BPY-MSN. The ¹³C CPMAS NMR spectra of the BPY-as-100 to BPY-as-350 series of samples are shown in Figure 2a. The chemical shifts observed after the heat

(38) Bennett, A. E.; Rienstra, C. M.; Auger, M.; Lakshmi, K. V.; Griffin, R. G. *J. Chem. Phys.* **1995**, *103*, 6951–6958.

(39) Burleigh, M. C.; Markowitz, M. A.; Spector, M. S.; Gaber, B. P. *Chem. Mater.* **2001**, *13*, 4760–4766.

Table 1. ^{13}C Chemical Shifts, Spectral Assignments, and Molecular Structures Identified in Functionalized MSN Materials

sample	spectral assignments ^a (δ_c given in ppm)	structure
BPY-MSN	C1: 14; C2: 24; C3: 44; C5: 167; C6: 143; C7: 121; C8: 149; C10: 157; C11: 123	
DMAP-MSN	C1: 11; C2: 23; C3: 55; C5: 36; C6: 155; C7,11: 108; C8,10: 151	
FPF-MSN	C1: 12; C2,3: 23; C4: 115; C5: 144; C6: 137; C7: 141; C8: 139; C9: 147	
MCM-as-100 (CTAB)	C1: 68; C2: 32; C3-14: 30; C15: 27; C16: 24; C17-19: 54	

^a As detailed in sections 3.1.1–3.1.3, the observed species also included the methoxy groups (at 50 ppm), ethoxy groups (at 16 and 58 ppm), and the products of CTAB decomposition following eqs 1–3.

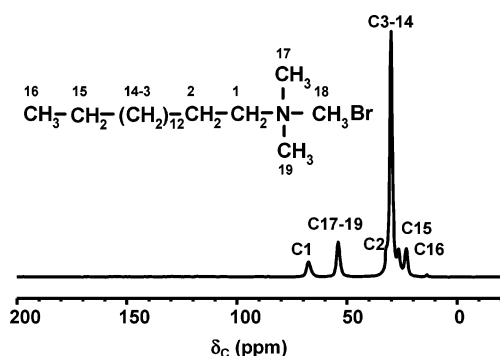
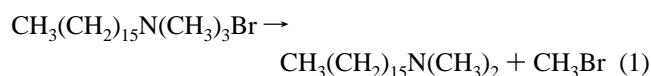


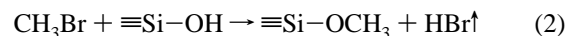
Figure 1. ^1H – ^{13}C CPMAS NMR spectrum of MCM-41-as-100. The resonances are assigned to CTAB, as shown.

treatment at 100 °C (sample BPY-as-100, top spectrum) represent BPY and CTAB, as marked in the figure. The resonances representing BPY remained unaffected by the increased severity of heating, whereas those due to CTAB, which overwhelmed the top spectrum, rapidly declined in intensity with increasing T_c . Initially, at temperatures below 200 °C, CTAB's structure remained intact, as evidenced by resonances at 68 (C1), 32 (C2), 30 (C3–14), 27 (C15), 24 (C16) and 54 ppm (C17–19), which are consistent with the ^{13}C CPMAS NMR spectrum of sample MCM-as-100 shown in Figure 1. However, in sample BPY-as-200, additional resonances appeared at 64 and 44 ppm, which at 225 °C took the place of those representing C1 and C17–19 in CTAB. Their presence is due to carbons C1, C17 and C18 in N,N -dimethylhexadecylamine ($\text{CH}_3(\text{CH}_2)_{15}\text{N}(\text{CH}_3)_2$), which is a product of the decomposition of CTAB at 200 °C



The resulting CH_3Br (boiling point = 4 °C) is either

evacuated or reacts with $\equiv\text{Si}-\text{OH}$ groups to form $\equiv\text{Si}-\text{OCH}_3$ and HBr according to



The validity of reaction 1 was directly confirmed through the analysis of the liquid residue that condensed during the evacuation on the wall of the glass tube containing the sample. The solution ^{13}C NMR spectrum of this residue in CDCl_3 (see spectrum S1a in the Supporting Information) is in exact agreement with the spectrum expected for $\text{CH}_3(\text{CH}_2)_{15}\text{N}(\text{CH}_3)_2$.^{40,41} In the case of reaction 2, HBr was most likely removed by evacuation, whereas the methoxy ($\equiv\text{Si}-\text{OCH}_3$) groups remained on the surface, as evidenced by the emergence of the resonance at 50 ppm in Figure 2a.

Thus, whereas CTAB does not exist in its intact form at $T_c \geq 200$ °C, the $\text{CH}_3(\text{CH}_2)_{15}\text{N}(\text{CH}_3)_2$ species persist inside some of the pores at a concentration level corresponding to about 5–10% of the initial CTAB concentration observed at $T_c = 100$ °C. This is illustrated in Figure 3a, which shows the sum of integrated intensities of all resonances representing CTAB and/or $\text{CH}_3(\text{CH}_2)_{15}\text{N}(\text{CH}_3)_2$ as a function of T_c . There are two possible explanations for this finding. The $\text{CH}_3(\text{CH}_2)_{15}\text{N}(\text{CH}_3)_2$ species may remain entrapped inside the silica matrix as a result of pore blockage during the heat treatment. The reduced pore volume per gram of materials after heating (see section 3.3) is in agreement with this hypothesis. Alternatively, these observed signals could be attributed to the $\text{CH}_3(\text{CH}_2)_{15}\text{N}^+\text{H}(\text{CH}_3)_2$ species. As depicted in eq 2, HBr was generated from the reaction between CH_3Br and surface silanols. It is foreseeable that HBr could

(40) Ganguly, S.; Roundhill, D. M. *Polyhedron* **1990**, *9*, 2517–2526.

(41) Ganguly, S.; Joslin, F. L.; Roundhill, D. M. *Inorg. Chem.* **1989**, *28*, 4562–4564.

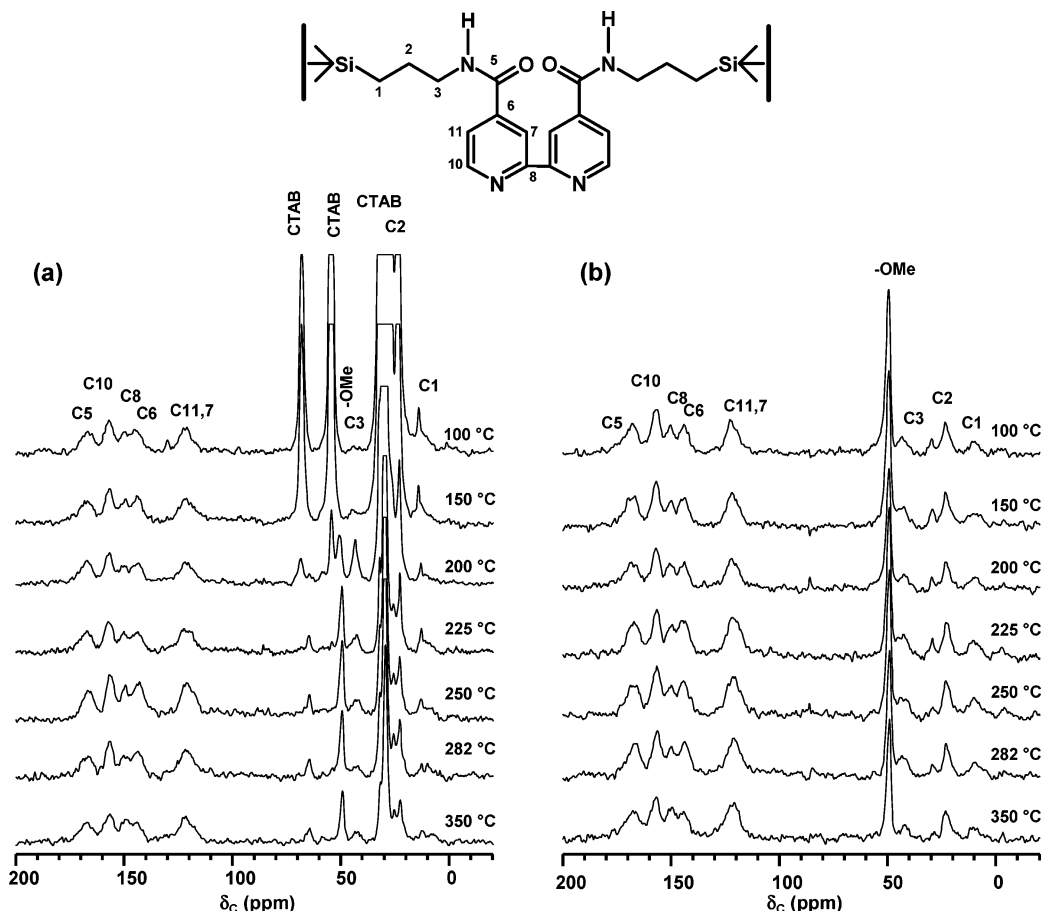


Figure 2. ^1H - ^{13}C CPMAS NMR spectra of (a) BPY-as and (b) BPY-ex series of samples following heat treatment at $100\text{ }^\circ\text{C} \leq T_c \leq 350\text{ }^\circ\text{C}$.

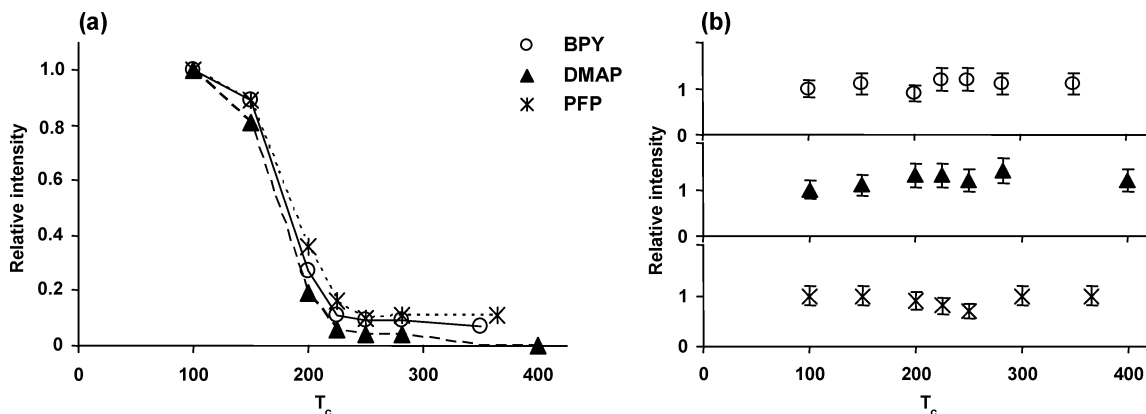


Figure 3. Concentrations of CTAB vs T_c in BPY-as, DMAP-as, and PFP-as series of samples (a), and of the organic functional groups in the corresponding BPY-ex, DMAP-ex, and PFP-ex samples (b). The experimental points represent integrated intensities of all ^{13}C resonances for each species. In the series of as-synthesized samples, the resonances representing CTAB were deconvoluted from those due to the coexisting functional groups.

protonate $\text{CH}_3(\text{CH}_2)_{15}\text{N}(\text{CH}_3)_2$ to give rise to the cationic $\text{CH}_3(\text{CH}_2)_{15}\text{N}^+\text{H}(\text{CH}_3)_2$ species that electrostatically binds to the surface silicate groups. Regardless of which scenario is operable, these residues did not affect the chemical properties of the organically functionalized BPY-MSNs, as detailed in section 3.2.

We note that these results are consistent with our earlier solid-state NMR study of nonfunctionalized MCM-41 silica nanoparticles.²⁹ Indeed, by using one- and two-dimensional ^1H , ^{13}C , and ^{29}Si experiments under 40 kHz MAS, we have demonstrated that the residual CTAB molecules, which were shown to remain inside the pores in the prone position along the channel walls, decomposed below $250\text{ }^\circ\text{C}$. Furthermore,

the ^1H peak representing CTAB's headgroup ($\text{N}(\text{CH}_3)_3$) was reduced at a faster rate as a function of T_c than the lines representing the CH_2 groups and the tail group (CH_3).²⁹

The spectra of BPY-ex series (Figure 2b) demonstrate that CTAB was completely removed by acid extraction. Indeed, only the resonances representing BPY are observed within the entire temperature range $100\text{ }^\circ\text{C} \leq T_c \leq 350\text{ }^\circ\text{C}$. Also present in the spectra is a peak at around 50 ppm, which we attributed to the methoxy groups produced during washing.

Further analysis of the functionalization of silicas was made by ^{29}Si NMR, which provided quantitative measurements of the concentrations of carbon-silicon bonds on the silica surface. The ^{29}Si DPMAS spectra of samples BPY-

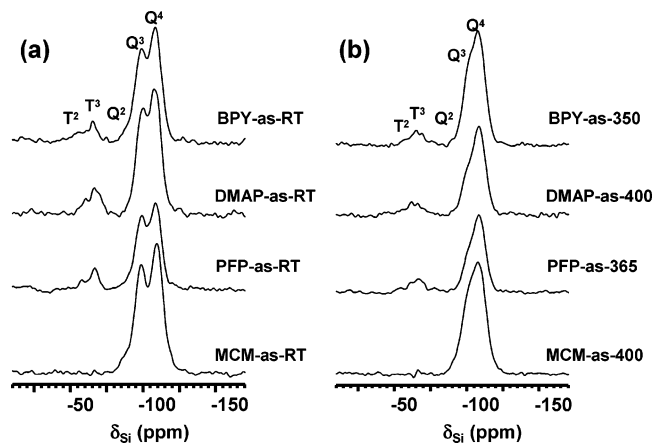


Figure 4. ^{29}Si DPMAS spectra of as-synthesized samples (a) prior and (b) after the heat treatment. Also shown are the corresponding spectra of nonfunctionalized samples MCM-41-as-RT and MCM-41-as-400.

as-100 and BPY-as-350 are shown in Figure 4. The functionalities of our interest, T^2 ($(\equiv\text{SiO})_2\text{Si}(\text{OH})\text{R}$) and T^3 ($(\equiv\text{SiO})_3\text{SiR}$), are well-known to resonate at around -56 and -67 ppm, respectively. Their presence in both spectra explicitly confirms the existence of covalent linkages between the silica surface and the organic groups in the entire T_c range. The resonance lines at around -92 , -99 , and -110 ppm represent silicon sites Q^2 ($(\equiv\text{SiO})_2\text{Si}(\text{OH})_2$, geminal silanol), Q^3 ($(\equiv\text{SiO})_3\text{SiOH}$, single silanol), and Q^4 ($(\equiv\text{SiO})_4\text{Si}$, siloxane), respectively.³⁶ The overall concentration ratio $T/Q = [(T^2 + T^3)/(Q^2 + Q^3 + Q^4)]$, along with the average molecular formulas and the molecular concentrations of organic functionalities (in mmol/g), which were all calculated using the integrated intensities of the ^{29}Si NMR spectra, are listed in Table 2. The fact that the T/Q ratio has remained essentially unchanged (within $\pm 5\%$) during the heat

Table 2. Quantification of the Silicon on the Basis of Deconvolution of ^{29}Si NMR Spectra of Figure 4

sample	T/Q ratio ^a	molecular formula (SiO_2) ₁₀₀ (H_2O) _m (R) _n	concentration of organic groups (mmol/g)
BPY-as-RT	0.12 (0.11)	(SiO_2) ₁₀₀ (H_2O) ₁₇ ($\text{C}_{18}\text{H}_{21}\text{N}_2\text{O}_2$) ₁₁	1.15
DMAP-as-RT	0.14 (0.14)	(SiO_2) ₁₀₀ (H_2O) _{16.5} ($\text{C}_9\text{H}_{14}\text{N}_2$) ₁₂	1.48
PFP-as-RT	0.13 (0.13)	(SiO_2) ₁₀₀ (H_2O) ₂₂ ($\text{C}_9\text{H}_7\text{F}_5$) ₁₂	1.54

^a Numbers in parentheses correspond to the samples calcined at the highest temperatures, BP-as-350, DMAP-as-400, and PFP-as-365, respectively.

treatment confirms that the BPY functional groups remain covalently bound to the silica surface. Remarkably, these functional groups persist on the surface despite considerable surface reconstruction due to dehydroxylation, which is evidenced by the decreased Q^3/Q^4 ratio.²⁹ These results were further corroborated by the analyses of chemical accessibility and reactivity of the bipyridine functional groups as described in section 3.2.

In summary, the spectra of Figure 2 and the corresponding integrated intensities (Figure 3) showed that CTAB was efficiently removed during the heat treatment, whereas the structure and concentration of BPY functionalities remained intact as a function of T_c .

3.1.2. DMAP-MSN. The ^{13}C CPMAS NMR spectra of the DMAP-as series of samples are shown in Figure 5a, and the observed carbon chemical shifts are assigned in Table 1 on the basis of our recent report.¹⁸ At $T_c = 200$ °C, we observed weak peaks at around 64, 44, and 50 ppm, which were earlier ascribed to $[\text{CH}_3(\text{CH}_2)_{15}\text{N}(\text{CH}_3)_2]$ and $\equiv\text{Si}-\text{OCH}_3$ species resulting from reactions 1 and 2. However, the removal of CTAB and $\text{CH}_3(\text{CH}_2)_{15}\text{N}(\text{CH}_3)_2$ from samples functionalized with DMAP proceeded more rapidly than in the BPY-as series. The spectra in Figure 5a demonstrate that more than

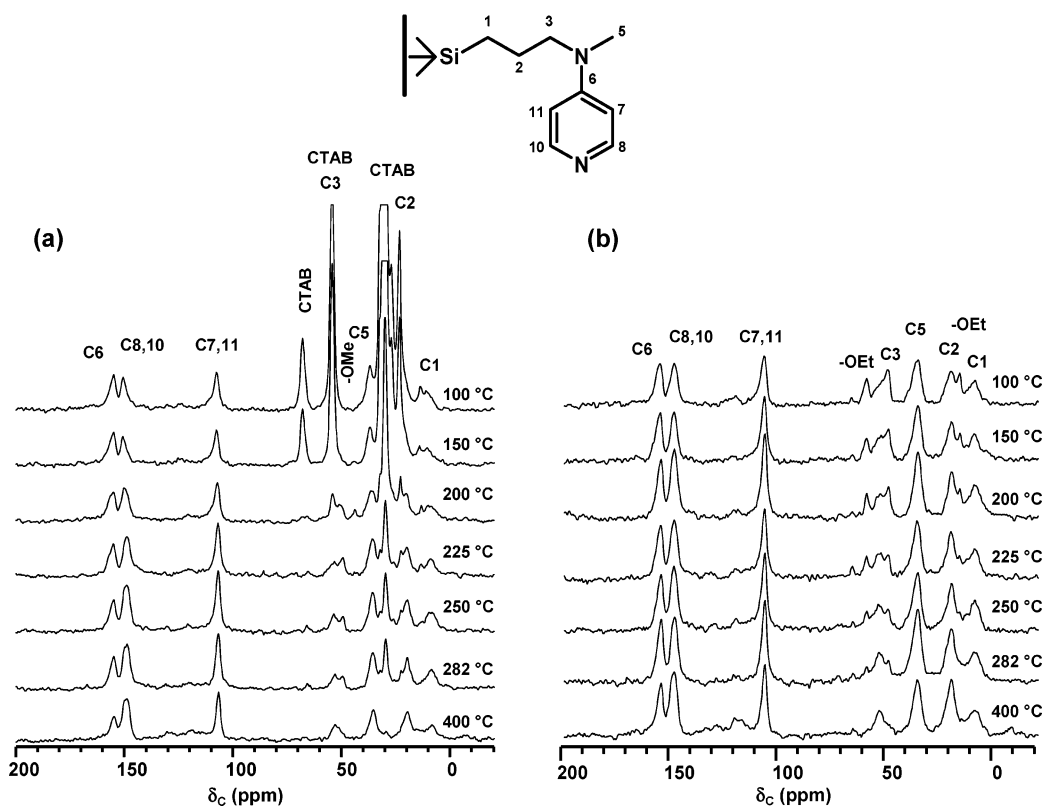


Figure 5. $^1\text{H}-^{13}\text{C}$ CPMAS NMR spectra of (a) DMAP-as and (b) DMAP-ex series of samples following thermal treatment at 100 °C $\leq T_c \leq 400$ °C.

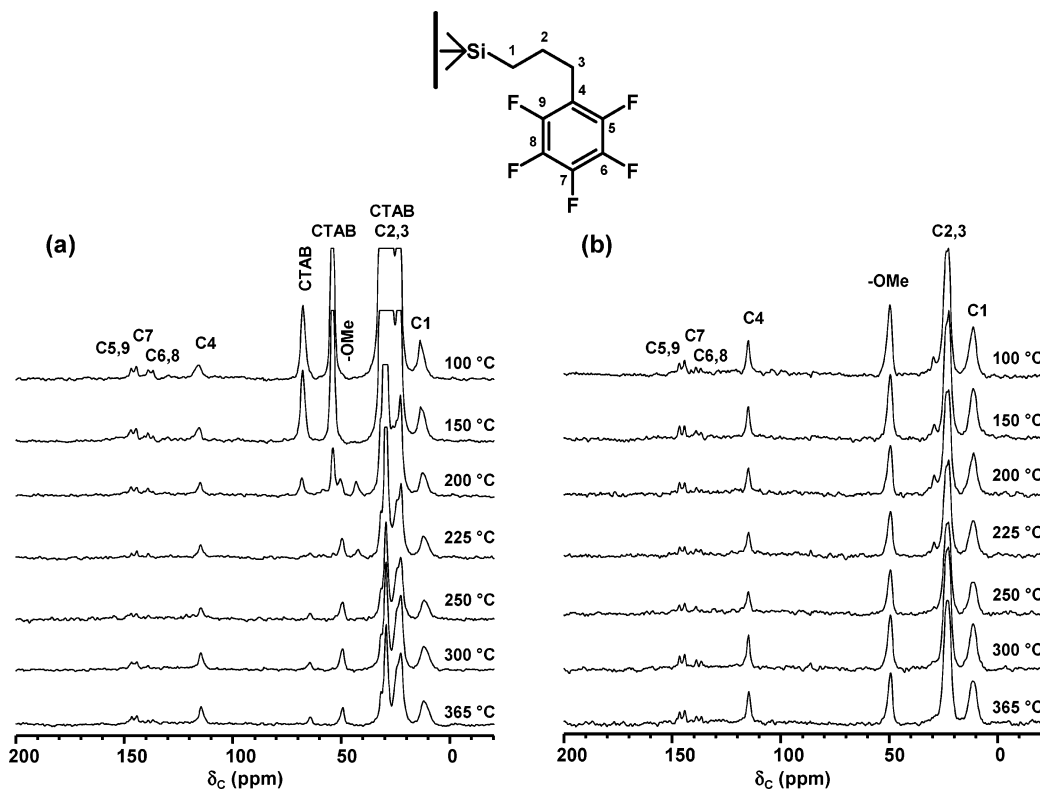


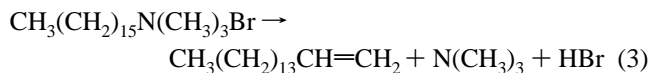
Figure 6. ^1H - ^{13}C CPMAS NMR spectra of (a) PFP-as and (b) PFP-ex series of samples following thermal treatment at $100\text{ }^\circ\text{C} \leq T_c \leq 365\text{ }^\circ\text{C}$.

90% of CTAB that was initially found in DMAP-as-100 was eliminated at $T_c = 225\text{ }^\circ\text{C}$. At $T_c = 400\text{ }^\circ\text{C}$, no detectable amount of the surfactant species was present, as further illustrated in Figure 3a. Again, our results show that DMAP functionalities appeared structurally intact during the heat treatment and maintained their initial concentration.

As in the case of BPY-MSNs, the spectra of DMAP-ex series of samples show that CTAB was completely removed by acid extraction (Figure 5b). However, two additional resonances were observed at around 58 and 16 ppm that represent the ethoxy groups ($\equiv\text{Si}-\text{OCH}_2\text{CH}_3$) that were produced from DMAP precursor during DMAP-MSN preparation. The concentration of DMAP as a function of T_c is shown in Figure 3b. The T/Q ratios obtained from the ^{29}Si DPMAS spectra of samples DMAP-as-RT and DMAP-as-400 (Figure 4 and Table 2) are in good agreement, thereby conclusively confirming the thermal stability of the functional groups.

3.1.3. PFP-MSN. The ^{13}C CPMAS NMR spectra of the PFP-as samples are shown in Figure 6a. Again, the observed carbon chemical shifts (see Table 1) confirm the presence of PFP functional groups inside the pores. The thermal extraction of CTAB and the products of its decomposition proceeds similarly to that in BPY-MSN and DMAP-MSN (see Figure 3a). The decomposition itself, however, follows two different routes. Here, also at $T_c = 200\text{ }^\circ\text{C}$, we discerned peaks at around 64, 44, and 50 ppm, assigned to tertiary amine ($\text{CH}_3(\text{CH}_2)_{15}\text{N}(\text{CH}_3)_2$) and $\equiv\text{Si}-\text{OCH}_3$ groups (see eqs 1 and 2). But the NMR analysis of liquid residue condensed during the evacuation at $T_c = 200\text{ }^\circ\text{C}$ showed that, in addition to the tertiary amine, resonances assigned to 1-hexadecene, $\text{CH}_3(\text{CH}_2)_{13}\text{CH}=\text{CH}_2$, were present (see spectrum S1b in the

Supporting Information). This implies that some of the CTAB molecules followed another route³⁵



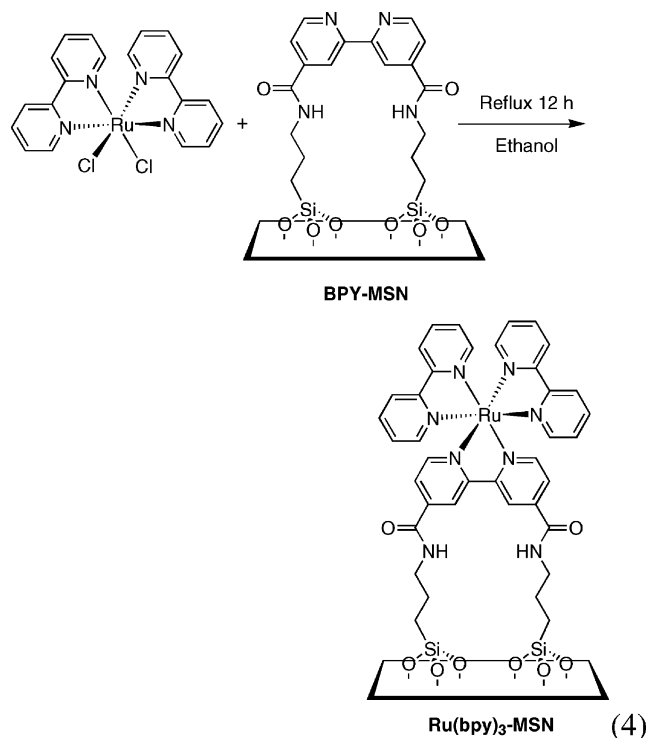
In the PFP-ex series, CTAB was completely removed by acid extraction as well. The spectra of Figure 6b show only the resonances representing PFP and a peak around 50 ppm, assigned to the methoxy groups from PFP-TMS. The concentration of PFP in the extracted sample as a function of T_c is shown in Figure 3b. Here also the T/Q ratios obtained from the ^{29}Si DPMAS spectra of samples PFP-as-RT and PFP-as-365 remain in a very good agreement (see Figure 4 and Table 2). (This may not be immediately obvious in Figure 4; note, however, that the intensity corresponding to Q^4 silicon sites increased considerably in sample PFP-as-365 at the expense of Q^3 .)

3.2. Chemical Accessibility and Catalytic Reactivity of Functional Groups in the Calcined and Extracted MSNs.

On the basis of the NMR results, it is plausible that some additional condensation of silica occurred in these MSNs during the heating process. The resulting structural changes could lead to the undesired entrapment of organic functional groups inside the silica matrixes, which would lower the chemical accessibility of the thermally treated MSNs with respect to the MSNs prepared by the conventional acid extraction method.

We first compared the chemical accessibility of 2,2'-bipyridine moieties in the calcined sample BPY-as-350 and acid-extracted sample BPY-ex-RT, by treating both materials

with excess $\text{Ru}(\text{bpy})_2\text{Cl}_2 \cdot x\text{H}_2\text{O}$ ethanol solution as shown in eq 4



The quantity of chemically accessible bipyridine functional groups in the BPY-MSN was determined by analyzing the decrease in $\text{Ru}(\text{bpy})_2\text{Cl}_2 \cdot x\text{H}_2\text{O}$ in solution, as described in section 2.5. The obtained concentrations, 34.8 and 35.9 $\mu\text{mol/g}$ of 2,2'-bipyridine in the BPY-as-350 and BPY-ex-RT, respectively, were significantly higher than the amount of physisorbed complexes measured on pure inorganic MCM-41 (20.9 $\mu\text{mol/g}$). The fluorescence spectra of treated BPY-as-350 and BPY-ex-RT showed a broad emission band, centered at 630 nm, representing the $\text{Ru}(\text{bpy})_3$ complexes. As expected, no fluorescence emission was detected in the physisorbed sample of pure MCM-41 (see the Supporting Information). It is noted, however, that the concentrations of functional groups obtained by this method were about 40 times lower than those measured by solid-state NMR (Table 2). A plausible explanation of this discrepancy is that $\text{Ru}(\text{bpy})_2\text{Cl}_2$ complexes are too large (1.15 nm) and too reactive to be used as a reliable probe of accessibility inside the pores with a diameter of about 2.5 nm (Table 4). Most likely, the complexation reaction that initiated near the pore entrances produced sufficient local concentrations of $\text{Ru}(\text{bpy})_3$ complexes to inhibit further diffusion of $\text{Ru}(\text{bpy})_2\text{Cl}_2$ molecules

Table 3. Catalytic Reactivity of DMAP-MSNs^a

sample	yield (%) ^b
DMAP-as-400	90
DMAP-ex-RT	99 ^c

^a Reaction conditions: 4-nitrobenzaldehyde (0.25 mmol), methyl vinyl ketone (0.5 mmol), and DMAP-MSN catalyst (50 mg, 30 mol %) in $\text{H}_2\text{O}/\text{THF}$ (2 mL, 1/3 v/v) at 50 °C for 24 h. ^b Isolated yield. ^c See ref 18.

Table 4. Structural Properties of Mesoporous Silica Nanoparticles

samples	S_{BET} (m^2/g) ^a	V_p (cm^3/g) ^a	W_{BJH} (Å) ^a	d_{100} (Å) ^b	a_0 (Å) ^b	$d_{\text{pore wall}}$ (Å) ^b
BPY-as-350	734.8	0.54	2.5	37.1	42.9	17.9
BPY-ex-RT	861.1	0.80	2.4	40.5	46.8	22.8
DMAP-as-400	686.3	0.33	2.0	32.7		
DMAP-ex-RT	834.5	0.39	2.0	32.2		
PFP-as-365	854.0	0.59	2.6	37.8	43.6	17.6
PFP-ex-RT	993.1	0.75	2.7	40.5	46.8	19.8

^a The BET surface area (S_{BET}), the mesopore volume (V_p), and the mean mesopore width (W_{BJH}) were obtained from the nitrogen adsorption/desorption data. ^b The d_{100} numbers represent the d -spacing corresponding to the main (100) XRD peak. The unit-cell size (a_0) is calculated from the d_{100} data using $a_0 = 2d_{100}/3^{1/2}$. The pore-wall thickness ($d_{\text{pore wall}} = a_0 - W_{\text{BJH}}$).

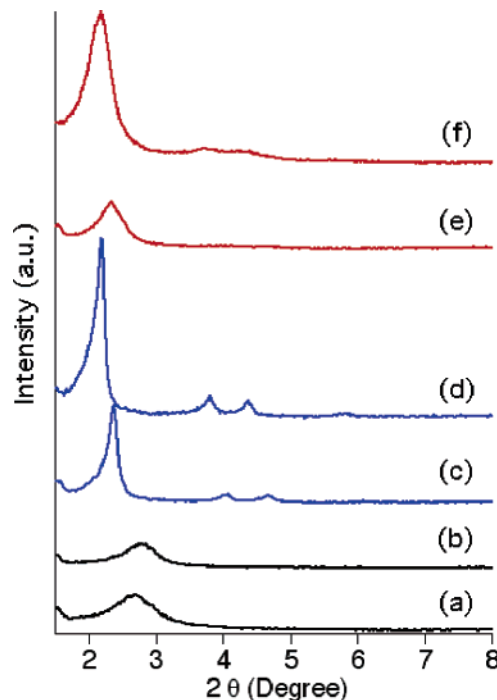


Figure 7. XRD spectra of (a) DMAP-as-400, (b) DMAP-ex-RT, (c) BPY-as-350, (d) BPY-ex-RT, (e) PFP-as-365, and (f) PFP-ex-RT.

into the channels. Therefore, we performed additional tests using a smaller molecule, $\text{Cu}(\text{NO}_3)_2$,^{11,12,39} which yielded the concentration of chemically accessible bpy groups of 0.28 mmol/g. This value, while still low, was exactly the same in BPY-as-350 and BPY-ex-RT samples. This strongly suggests that chemical properties of the organically functionalized MSNs obtained by our heating method remained unchanged.

To examine the catalytic reactivity after the heat treatment, a Baylis–Hillman reaction of 4-nitrobenzaldehyde and methyl vinyl ketone was conducted using DMAP-MSNs as catalysts. As shown in Table 3, the reaction catalyzed by DMAP-as-400 gave rise to a 90% yield, which was very similar to the yield obtained by the acid-extracted DMAP-ex-RT. This result confirmed that the chemical fidelity of the catalytic groups was indeed preserved in the calcined DMAP-MSN.

3.3. Textural Properties of the Calcined and Acid-Extracted MSNs. In addition to NMR, several structural characterization methods, including powder X-ray diffraction (PXRD), nitrogen adsorption/desorption experiment, and scanning electron microscopy (SEM), were used to further

examine the physical properties of the calcined and acid-extracted MSNs. The results were summarized in Table 4. As depicted in Figure 7, DMAP-MSN materials showed a disordered mesoporous structure as reported in our previous paper,¹⁸ whereas BPY-as-350 and PFP-as-365 materials exhibited the MCM-41 type, hexagonally packed mesopores, as indicated by (100), (110), and (200) peaks. The diffraction peaks of the calcined BPY-as-350 and PFP-as-365 were slightly shifted to a higher angle than those of the acid-extracted samples, indicating the formation of a smaller unit cell (a_0). The measured BET surface areas of the calcined MSNs were lower than those of the acid-extracted samples. As shown in the Supporting Information, type IV isotherms of N₂ sorption were observed in the calcined MSN materials, further confirming the cylindrical pore structures. The mean pore width of the calcined and acid-extracted MSNs, measured by BJH pore distribution, showed no significant difference. These results indicated that the calcined samples possess a thinner pore wall in comparison with those of the acid-extracted ones, which could be attributed to further condensation of the silica framework during the heating process. It is finally noted that both the calcined and acid-extracted MSNs showed similar particle morphologies as depicted in the SEM micrographs (see the Supporting Information).

4. Conclusion

In summary, we have investigated the thermal stability of three types of organically functionalized mesoporous silica

nanoparticles synthesized via the co-condensation method. The as-synthesized, surfactant-containing samples were thermally treated between 100 and 400 °C under vacuum, and the resulting materials were analyzed by solid-state NMR spectroscopy. We have demonstrated that the CTAB template molecules could be effectively removed from the mesopores while fully preserving the chemical fidelity of the organic functional groups by controlling the temperature. The chemical accessibility and reactivity of the organic functionalities were also conserved after the heat treatments. We envision that this temperature-controlled heating process could be further developed into an economical and environmentally friendly method for surfactant-removal of various organically functionalized mesoporous silica materials.

Acknowledgment. Support for this research work at Ames Laboratory through the U.S. DOE, Office of Basic Energy Sciences, through Catalysis Science Grant AL-03-380-011 and under Contract W-7405-Eng-82 is gratefully acknowledged. The authors express appreciation to Dr. J. W. Wiench for his assistance with the experiments and helpful comments.

Supporting Information Available: ¹³C solution NMR spectra of the liquid residues collected during the heat treatment of as-synthesized samples at 225 °C (S1), N₂ sorption analyses (S2), SEM micrographs (S3), and fluorescence spectra (S4). This material is available free of charge via the Internet at <http://pubs.acs.org>.

CM060598V